# Acute Modulation of Albumin Microvascular Leakage by Advanced Glycation End Products in Microcirculation of Diabetic Rats In Vivo

**Evelyne Bonnardel-Phu, Jean-Luc Wautier, Ann Marie Schmidt, Cecilia Avila, and Eric Vicaut**

**Advanced glycation end products (AGEs) are nonenzymatic glycosylated adducts of proteins that accumulate in vascular tissue during diabetes and aging. The aim of this work was to study the role of AGEs and of the oxidative mechanisms in diabetes-induced changes in vascular permeability. Intravital videomicroscopy was used to study albumin microvascular leakage in cremaster muscle. The extravasation of a fluorescent macromolecular tracer (fluorescein isothiocyanate-albumin) was measured for 1 h and, after computer-aided image analysis, was expressed as variations of normalized gray levels (arbitrary units). Extravasation of the macromolecular tracer was much higher in diabetic rats than in control rats (slope of extravasation versus time increased by >100%, $P < 10^{-4}$). This increase was significantly inhibited when we blocked AGEs binding to their endothelial receptor by intravenous bolus of soluble recombinant receptor to AGEs (rR-RAGE) (slope of extravasation versus time decreased by 19, 30, and 40%, for 0.5, 2.5, and 5.15 mg/kg rR-RAGE, respectively) or by a 6 mg/kg intravenous bolus of antibody against RAGE (slope decreased by 53%). Systemic injection of probucol (an antioxidant) also significantly inhibited the increase in the extravasation of the macromolecular tracer occurring in experimental diabetes (slope decreased by 51%, $P < 10^{-4}$). These results strongly suggest that in experimental diabetes the interaction of circulating AGEs and endothelial RAGE mediates albumin micro-vascular leakage, possibly via AGE-RAGE–dependent enhanced oxidant stress. *Diabetes* 48:2052–2058, 1999**

From the Microvascular Research Laboratory (E.B.-P., E.V.), Department of Biophysics, F. Widal Hospital; the Laboratory of Cellular and Vascular Biology Paris 7 (J.-L.W.), National Institute of Blood Transfusion, Paris, France; and the College of Physicians and Surgeons (A.M.S., C.A.), Columbia University, New York, New York.

Address correspondence and reprint requests to Pr. Eric Vicaut, Laboratoire d'Etude de la microcirculation, Département de Biophysique, Hôpital F. Widal, 200 rue du Faubourg Saint Denis, 75475 Paris Cedex 10, France. E-mail: eric.vicaut@lrb.ap-hop-paris.fr.

Received for publication 4 December 1997 and accepted in revised form 15 June 1999.

AGE, advanced glycation end product; $A\%_{tiss}$, percentage of non-vascular tissue area; $A\%_{vasc}$, percentage of vascular tissue area; FITC, fluorescein isothiocyanate; GL, gray level; PCD, perfused capillary density; RAGE, receptor for AGE; rR-RAGE, recombinant rat receptor for AGE; STZ, streptozotocin.

An increase in transvascular passage of macromolecules is observed in diabetes (1). Such a phenomenon has been described in different types of diabetes in animals (2,3) and was also found in patients (4–6) even at an early stage of the disease (7).

Several mechanisms have been proposed to explain this increase in passage of transvascular macromolecules associated with diabetes. Hemodynamic changes, inducing an increase in capillary pressure, have been demonstrated in some diabetic patients (8). Changes in capillary permeability can also result from several mechanisms, including release of humoral mediators known to affect microvascular permeability such as kinins (9), histamine, or serotonin (10). Alterations in prostanoid balance can also increase microvascular permeability. The role of changes in nitric oxide synthesis is still debated (11,12).

Because it has been demonstrated that advanced glycation end products (AGEs) have cellular receptors (RAGEs) on endothelial cells, smooth muscle cells, and macrophages (13), increased production of AGEs has been suggested as a link between hyperglycemia and diabetic vasculopathy. Indeed, it has been shown that in diabetic vasculature from both animals and diabetic patients, increased expression of RAGE colocalizes with strikingly increased deposition/formation of blood vessel AGEs (14–17). AGE–RAGE interaction can induce an oxidant stress in the vasculature (18,19), which could play a role in diabetic vasculopathy (20,21). Increased oxidative stress at the endothelial level by increased production or decreased destruction of free radicals (22) may also directly or indirectly affect capillary permeability. Furthermore, we observed an effect of AGEs on vascular permeability in diabetes as determined by measurements of whole-organ permeability (23).

In the present study we used intravital microscopy for a direct in vivo evaluation of the role of AGE binding to endothelial RAGE in albumin microvascular leakage in streptozotocin (STZ)-induced diabetes. For this purpose we inhibited the binding by using a soluble form of recombinant RAGE (rR-RAGE), a truncated protein composed of an extracellular domain of the membrane-anchored receptor (13), or by blocking the receptor with a specific anti-RAGE antibody. In addition, we tested the hypothesis that the increase in albumin microvascular leakage in this experimental model of diabetes can be linked to an increase in reactive oxygen intermediates production at the microvascular level, secondary to the binding of AGE to RAGE.

## RESEARCH DESIGN AND METHODS

**Induction of diabetes.** Three-week-old male Wistar rats (CERJ, Laval, France) were rendered diabetic by intraperitoneal injection of 70 mg/kg STZ in a citrate buffer. The development of diabetes was assessed two weeks after injection by blood glucose measurements (Peridochrom Glucose Kit; Boehringer Mannheim, Libourne, France). Blood was drawn under light ether anesthesia from the retro-orbital sinus.

**Experimental setup.** The animals used in this study had a diabetes duration of 7 weeks. They were anesthetized with 30 mg/kg pentobarbital sodium (Sanofi, Paris). During the experiments, rat temperature was maintained at 37°C with a thermostated heating pad. A tracheotomy was performed to facilitate spontaneous breathing. The carotid artery was cannulated for measurement of systemic mean arterial blood pressure and the jugular vein was cannulated for tracer and drug injection. If an animal's mean blood pressure fell to <80 mmHg during the surgical preparation procedure, it was excluded from the study.

**Preparation of the cremaster.** The right cremaster muscle was surgically prepared for in vivo visualization by a technique described in detail elsewhere (24). Briefly, the muscle was detached from the scrotum and a transverse buttonhole slit about 5 mm long was made in the proximal part of the cremaster pouch. The testicle and epididymis and the cremaster itself were then drawn out through the buttonhole. This procedure led to the invagination of the cremaster, which acquired a finger shape, with the cremaster pouch now turned inside out. The small pedicle that attaches the cremaster to the testicle was tied with two stitches and cut between them, to separate the cremaster completely from the testicle, which was removed. To prepare the cremaster muscle for epi-illumination microscopy, a thin black plate was introduced longitudinally into the cremaster pouch, to eliminate background reflection. The plate had been positioned so that the main cremaster artery was in the center of the plate's upper surface. Throughout these procedures, the muscle was continuously bathed with warm saline solution.

This preparation procedure involves minimal incision of the cremaster and so reduces considerably the risk of hemorrhage and of lesions to the muscle and its microcirculation. Because the size of the black plate is adapted to the dimensions of the cremaster, the extension of the muscle is sufficient to allow good optical resolution, but does not affect the microcirculation.

The muscle was continuously superfused at 2 ml/min with a modified Ringer solution bubbled with a 6% $CO_2$/94% $N_2$ gas mixture and containing 136.8 mmol/l NaCl, 4.7 mmol/l KCl, 1.2 mmol/l $CaCl_2$, 2.4 mmol/l $MgSO_4$, 25 mmol/l $NaHCO_3$, and 30 mmol/l HEPES at a temperature of 34–35°C in the muscle chamber.

To visualize the microcirculation, the chamber was placed on the movable stage of a modified Leitz microscope and the cremaster muscle was epi-illuminated using a 50-W mercury lamp. The image, magnified by a 2.5× objective and 10× oculars, was projected into a high-performance CCD camera (COHU) connected to a professional videotape recorder (S-VHS, NVFS 100 HQ; Panasonic, Japan). During the experiments, all automatic gain control was disabled, and the same gain was used for every experiment.

After a 15-min stabilization period, fluorescein isothiocyanate (FITC)-albumin (250 mg/kg) was administered by an intravenous bolus, and the preparation was allowed to stabilize an additional 15 min. In case of spontaneous leakage, the experiment was discarded. Otherwise, after the 15-min stabilization period, image was video-recorded every 10 min for 1 h. The same area of tissue was followed over time in each experiment. The period of observation was limited to 1 h because in preliminary experiments an increase in permeability was observed in control animals after 1 h, due to surgical exposure of the muscle. This artifact corresponds to a nonlinear fluorescence-versus-time relationship, while no significant nonlinearity was found in the period of observation used in the present experiments.

**Albumin microvascular leakage measurements.** Transport of albumin across microvascular wall was measured by playback analysis of the video records: fluorescence intensities in the intravenular and corresponding perivascular area were measured as a function of time, using a computer-assisted digital imaging processor (NIH 1.57 on a Macintosh Centris 660 AV computer). Each digitized image (~17,000 square pixels) was comprised of pixels with gray scale values ranging from 0 (white) to 255 (black) (25).

In a preliminary study, using solutions of FITC-albumin in a range of concentrations corresponding to the range of concentrations observed in in vivo experiments, we established that the relationship between concentration of FITC-labeled albumin and the gray level (GL) values was linear, with a regression coefficient of 0.983.

For each experiment, at $t_0$ only vessels were fluorescent, thus giving a histogram of pixel values distribution limited to the values obtained in vessels (low pixel values) and those in nonvascular tissue (high pixel values). The range of pixel values ($\Delta GL_{max}$) in the image recorded at $t_0$ corresponded to the maximal changes in fluorescence that might occur in a particular experiment and was calculated for each muscle. From the histogram of repartition of pixels in the image at $t_0$, we also calculated the percentage of vascular ($A\%_{vasc}$) and nonvascular tissue areas ($A\%_{tiss}$) in the studied area.

Then, for each time, we measured the average GL in the studied area.

The average GL of the studied area corresponded to the average of GL in vessels and in nonvascular tissue weighted by $A\%_{vasc}$ and $A\%_{tiss}$ in the studied area, i.e., $(GL_{total\ image} \times 100) = (GL_{vessels} \times A\%_{vasc}) + (GL_{tissue} \times A\%_{tiss})$.

Thus the average GL corresponding to the fluorescence in the nonvascular tissue areas corresponding to the transport of albumin across microvascular wall can be calculated as:

$$GL_{tissue} = \frac{(GL_{total\ image} \times 100) - (GL_{vessels} \times A\%_{vasc})}{A\%_{tiss}}$$

Then, changes in fluorescence in the tissue were expressed as a function of time, and normalized in arbitrary units (AU) by the following formula:

$$\%\ GL_{tissue} = \frac{GL_{tissue}(t_0) - GL_{tissue}(t)}{\Delta GL_{max}} \times 100$$

where $t_0$ is the first measurement, and $t$ is 10, 20, 30, 40, 50, or 60 min.

The changes in $\%\ GL_{tissue}$ with time reflected the accumulation of albumin within the tissue; the slope of this relationship is a transport rate that is dependent on permeability. It should be noted that in our experiments, these measurements reflected macromolecule leakage in a given area of measurement, i.e., in a given volume of muscle. However, because diabetic rats had a lower weight than control animals (223 vs. 394 g on average), it was possible that the cremaster muscle was thinner for diabetic rats, and that the corresponding volume differed. For this reason, the measurements of fluorescence intensity were normalized by the value of dry weight of cremaster.

**Preparation of rR-RAGE and anti-RAGE antibodies**

***Cloning expression and purification of rR-RAGE.*** rR-RAGE was obtained as previously described (23). Full-length rR-RAGE CDNA was cloned by screening a lung CDNA library. A DNA fragment coding for soluble RAGE was obtained using polymerase chain reaction with specific primers. Baculovirus expression of rR-RAGE was performed by cotransfecting the plasmid p.Bac PAK8/RAGE into *Sf*9 cells. rR-RAGE was purified by chromatography to obtain a homogeneous sample of 35 KDa on SDS-PAGE. This protein corresponds to the expected extracellular domain. rR-RAGE binds AGE ligands and competes with cell-surface RAGE for AGE cell binding (23). Pharmacokinetics of rR-RAGE in plasma of diabetic rats has been recently characterized as a biexponential distribution model with average half-lives equal to 0.15 and 4.01 h and elimination half-life equal to 57.17 h (26).

***Anti-RAGE antibodies.*** Anti-RAGE antibodies were obtained in rabbit and were purified as previously described (18). Anti-RAGE antibodies were prepared against human RAGE but cross-reacted with rat RAGE. The anti-RAGE antibodies were injected in animals as an IgG fraction sterilized by filtration and were endotoxin-free.

**Experimental protocols**

***Evaluation of the effect of diabetes on albumin microvascular leakage in the experimental model.*** Three groups of rats were studied: a group of diabetic rats ($n = 6$) 7 weeks after diabetes induction, a group of normoglycemic rats ($n = 5$) matched by age with the diabetic rats, and a group of normoglycemic rats ($n = 6$) matched by weight with diabetic rats.

In a complementary series of experiments, we compared perfused capillary density (PCD) in diabetic and in age-matched normoglycemic rats ($n = 5$ in each group). PCD was estimated by counting the number of capillaries that contained moving red cells and intersected a horizontal line 150 µm in length on the video monitor after optical positioning of the video image so that the image of most capillaries was vertical. From 5 to 7 contiguous fields were studied in each rat.

***Inhibition of diabetes-induced increase in albumin microvascular leakage by rR-RAGE.*** Six groups of rats were studied. Diabetic rats were allocated to receive either rR-RAGE (0.5, 2.5, or 5.15 mg/kg, $n = 7$, 5, and 5, respectively) or saline ($n = 13$) by intravenous bolus 1 h before the beginning of the experiment. In addition, we studied age-matched normoglycemic rats allocated to receive under the same conditions either rR-RAGE (5.15 mg/kg, $n = 3$) or saline ($n = 13$).

In a complementary series of experiments ($n = 3$ rats in each group), we injected rR-RAGE (5.15 mg/kg) 15 min, 3 h, or 12 h before the beginning of the experiments to explore the kinetics of the effect.

***Inhibition of diabetes-induced increase in albumin microvascular leakage by anti-RAGE antibodies.*** Anti-RAGE (6 mg/kg in 0.5 ml by intravenous bolus) or saline was administered to diabetic ($n = 5$ and 11, respectively) and age-matched normoglycemic rats ($n = 3$ and 13, respectively) 1 h before the beginning of the experiment.

***Inhibition of diabetes-induced increase in albumin microvascular leakage by probucol.*** Probucol was infused intravenously 1 h before the beginning of the experiment in diabetic and age-matched normoglycemic rats (30 µg/kg, dissolved in 1% ethanol, 0.3 ml i.v., $n = 6$ in each group); saline was infused in 10 diabetic and 15 age-matched normoglycemic rats. The dose of

TABLE 1
Body weight and blood glucose levels of untreated and treated diabetic and normoglycemic rats

| | Initial body weight (g) | Final body weight (g) | Glycemia (mmol/l) |
|---|---|---|---|
| Diabetic rats | 65 ± 3 | 191 ± 17 | 26.3 ± 1.6 |
| Weight-matched controls | 61 ± 2 | 231 ± 18 | 7.7 ± 1.6 |
| Age-matched controls | 60 ± 2 | 378 ± 13 | 8.5 ± 0.3 |
| rR-RAGE treatment | | | |
| Untreated diabetic rats | 60 ± 2 | 228 ± 16 | 25.8 ± 1.1 |
| rR-RAGE–treated diabetic rats | | | |
| 5 mg/kg | 60 ± 2 | 223 ± 20 | 27.2 ± 1.7 |
| 2.5 mg/kg | 59 ± 2 | 185 ± 17 | 26.2 ± 0.9 |
| 0.5 mg/kg | 60 ± 2 | 192 ± 11 | 23.1 ± 1.3 |
| Controls | | | |
| Untreated | 66 ± 3 | 393 ± 8 | 8.6 ± 0.3 |
| rR-RAGE–treated | 60 ± 1 | 353 ± 37 | 8.8 ± 0.1 |
| rR-RAGE pretreatment | | | |
| Untreated diabetic rats | 103 ± 2 | 275 ± 18 | 31.4 ± 5.7 |
| rR-RAGE–pretreated diabetic rats | | | |
| 15 min | 60 ± 4 | 220 ± 60 | 30.7 ± 3.2 |
| 3 h | 108 ± 4 | 312 ± 60 | 30.8 ± 4.4 |
| 12 h | 110 ± 1 | 239 ± 33 | 36.3 ± 4.0 |
| Anti-RAGE treatment | | | |
| Untreated diabetic rats | 58 ± 2 | 188 ± 24 | 26.1 ± 0.6 |
| Anti-RAGE–treated diabetic rats | 67 ± 3 | 251 ± 19 | 25.5 ± 1.1 |
| Untreated controls | 72 ± 7 | 386 ± 22 | 11.6 ± 2.5 |
| Anti-RAGE–treated controls | 76 ± 2 | 360 ± 10 | 7.6 ± 0.6 |
| Probucol treatment | | | |
| Untreated diabetic rats | 60 ± 2 | 206 ± 12 | 28.5 ± 1.2 |
| Probucol-treated diabetic rats | 62 ± 1 | 220 ± 20 | 28.3 ± 3.2 |
| Untreated controls | 64 ± 3 | 398 ± 11 | 9.8 ± 1.1 |
| Probucol-treated controls | 68 ± 7 | 412 ± 17 | 9.1 ± 0.8 |

Data are means ± SE. Initial body weight of rats is not different among the groups. Diabetic rats have significantly elevated plasma glucose levels and significantly lower final body weight. There is no difference between treated or untreated diabetic groups for these parameters.

probucol was chosen on the basis of its efficacy in inhibiting oxidative stress in in vitro experiments (23).

In all experiments, we compared the difference in albumin transport across the microvascular wall, reflected by the fluorescence changes versus time for the different groups of rats in each set of experiments.

**Drugs.** If not specified, drugs were purchased from Sigma-Aldrich (Saint Quentin Fallavier, France). Albumin used was a standardized FITC-albumin (FITC content 12 mol/mol albumin) prepared from crystallized and lyophilized bovine albumin by Sigma. Note that the batch of fluorescent albumin used in the first set of experiments was different from that used for the two others.

**Immunohistochemistry.** Cremaster muscles were obtained from diabetic or age-matched control rats and fixed overnight with 4% paraformaldehyde then washed with PBS, dehydrated, and embedded in paraffin by standard procedures. Immunohistochemical studies used sections that were rehydrated, and final concentration of the anti-RAGE IgG was 3 μg/ml.

**Statistical analysis.** All data obtained in this study were expressed as means ± SE. To assess the statistical significance of differences between groups, two-way analysis of variance, with one between factors (group) and one within factor (time), was utilized. Slopes of fluorescence versus time were estimated by regression analysis. The level of significance was fixed at 5%. Software Statview 4.5 (Abacus Concepts) was used for calculation.

## RESULTS

Rat body weight, and blood glucose level of normoglycemic or diabetic rats treated or untreated, are shown in Table 1. Weight was significantly lower in the diabetic compared with the normal rats. Glycemia was about threefold higher in the diabetic animals. No significant difference for these parameters was found between treated and untreated animals. Mean blood pressure was equal to 119 ± 3 mmHg and was similar in the different groups of rats.

**Evaluation of the effect of diabetes on albumin microvascular leakage in the experimental model.** As shown in Fig. 1, analysis of the time-course of average optical intensity showed that extravasation of FITC-albumin was significantly higher in diabetic than in nondiabetic rats ($P < 10^{-4}$). No significant difference was found between weight-matched and age-matched control groups.

Indeed, the slope of the curve for fluorescence versus time (considered as an estimation of the transport rate) was more than twofold higher in diabetic compared with nondiabetic rats (0.073 in diabetic vs. 0.030 and 0.035 in weight-matched and age-matched nondiabetic rats).

The number of capillaries perfused in the normal and diabetic rats (31.4 ± 2.1 vs. 29.2 ± 1.4 capillaries/mm of field) was similar (NS).

**Inhibition of diabetes-induced increase in albumin microvascular leakage by rR-RAGE.** As shown in Fig. 2., extravasation of fluorescent albumin was significantly different among the six groups of rats studied ($P < 10^{-4}$). In diabetic rats rR-RAGE was found to reduce in a dose-dependent fashion FITC-albumin extravasation. The slope of the curve for fluorescence versus time was 0.135 for untreated diabetic rats and 0.109, 0.095, and 0.079 for diabetic rats treated with 0.5, 2.5, and 5.15 mg/kg rR-RAGE, respectively. The slopes were equal to 0.032 and 0.046 for untreated normoglycemic and rR-RAGE–treated normoglycemic rats. At the highest dose tested (5.15 mg/kg) the difference with the untreated diabetic

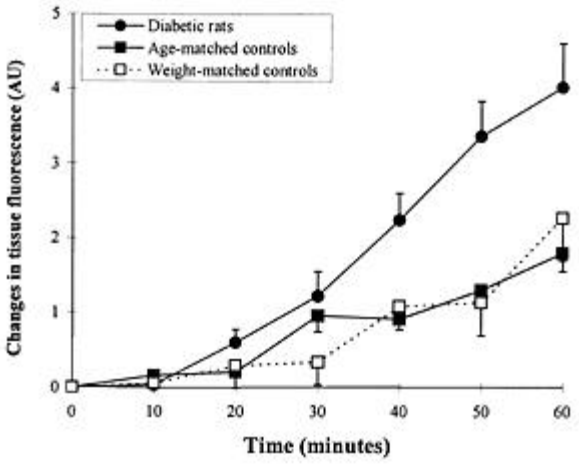


**FIG. 1. Comparison of changes in microvascular albumin leakage in diabetic rats and in age-matched or weight-matched controls. Diabetic rats and age-matched controls were studied 7 weeks after injection of STZ (70 mg/kg) or citrate buffer. Weight-matched controls were 4 weeks younger. After 1 h, FITC-albumin extravasation was increased twofold in diabetic rats, compared with both controls. The results are presented as means ± SE, with $n$ = 5 for age-matched controls and $n$ = 6 for weight-matched controls and diabetic rats.**

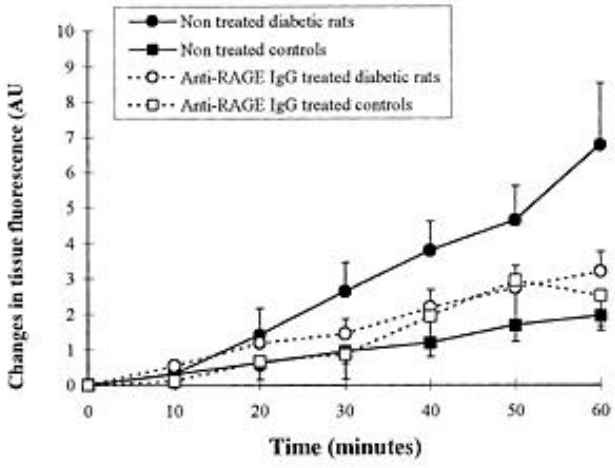


**FIG. 3. Effects of an intravenous bolus of anti-RAGE IgG on diabetes-induced increases of microvascular albumin leakage. Diabetic and age-matched normoglycemic rats were allocated to receive either anti-RAGE IgG (6 mg/kg in 0.5 ml, $n$ = 5 and 3, respectively) or saline ($n$ = 11 and 13, respectively), 1 h before the beginning of the experiment. Anti-RAGE IgG partially inhibited the increase in FITC-albumin extravasation observed in diabetic rats ($P < 10^{-4}$).**

rats reached the level of significance ($P < 0.05$). Despite a trend for higher albumin extravasation in 5.15 mg/kg–treated diabetic rats than in untreated normoglycemic rats, the difference between these two groups did not reach significance. In addition, no significant difference was found between untreated and rR-RAGE-treated normoglycemic rats.

When we analyzed the results of the kinetics of rR-RAGE, we did not find any significant difference between the curves of fluorescence versus time observed in diabetic rats either 1 h or 3 h after the injection. In addition, the results of these two groups were significantly different ($P < 0.05$) from those

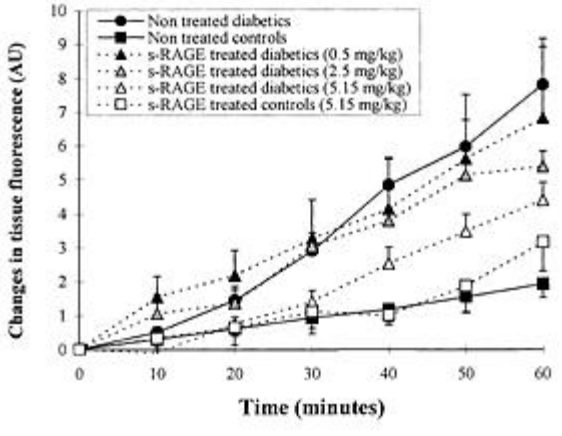


**FIG. 2. Effects of rR-RAGE on diabetes-induced increases in microvascular albumin leakage. Diabetic rats and age-matched controls were studied 7 weeks after injection of STZ (70 mg/kg) or citrate buffer. Before the experiment, diabetic rats were assigned to untreated or rR-RAGE–treated groups (0.5, 2.5, and 5.15 mg/kg). There was no difference in glycemia levels and animals' weight between these groups. In diabetic rats, rR-RAGE was found to reduce in a dose-dependent fashion FITC-albumin extravasation. At the highest dose tested (5.15 mg/kg), the difference with the untreated diabetic rats reached the significance level ($P < 0.05$). The results are presented as means ± SE, with $n$ = 11, 7, 5, and 5 for the untreated, 0.5 mg/kg, 2.5 mg/kg, and 5.15 mg/kg treated diabetic rats, respectively, and $n$ = 13 and 3 for untreated and 5.15 mg/kg rR-RAGE–treated controls, respectively.**

of the untreated diabetic rats and not significantly different from the normoglycemic rats. No significant inhibition of microvascular hyperpermeability was found in diabetic rats either very shortly after injection (i.e., 15 min) or 12 h after injection. For these two groups, the curves for fluorescence versus time were significantly different from those found in normoglycemic rats ($P < 0.05$) and nonsignificantly different from those found in untreated diabetic rats.

**Inhibition of diabetes-induced increase in albumin microvascular leakage by anti-RAGE antibodies.** As shown in Fig. 3, extravasation of fluorescent albumin was significantly different in the four groups of rats ($P < 10^{-4}$). The slopes of the curves for fluorescence versus time were equal to 0.112 for untreated diabetic rats vs. 0.053 for the anti-RAGE–treated diabetic rats. The slopes were equal to 0.006 for the untreated normoglycemic rats and 0.051 for anti-RAGE–treated normoglycemic rats.

In diabetic rats treated by blocking AGE binding to endothelial RAGE with anti-RAGE, we found a significantly lower FITC-albumin extravasation than in untreated diabetic rats. Despite a trend for a higher albumin extravasation in treated diabetic rats than in untreated normoglycemic rats, the difference between these two groups did not reach the significance level. No significant difference was found between normoglycemic rats receiving or not receiving anti-RAGE antibodies.

**Inhibition of diabetes-induced increase in albumin microvascular leakage by probucol.** As shown in Fig. 4, extravasation of fluorescent albumin was significantly different in the four groups of rats ($P < 10^{-4}$). In diabetic rats treated with probucol we found a significantly lower FITC-albumin extravasation than in untreated diabetic rats. No significant difference was found between treated diabetic, control normoglycemic, and treated normoglycemic rats.

The slopes of the curves for fluorescence versus time were equal to 0.151 and 0.074 for the diabetic and diabetic-treated rats and to 0.036 and 0.045 for the normoglycemic and normoglycemic-treated rats, respectively.

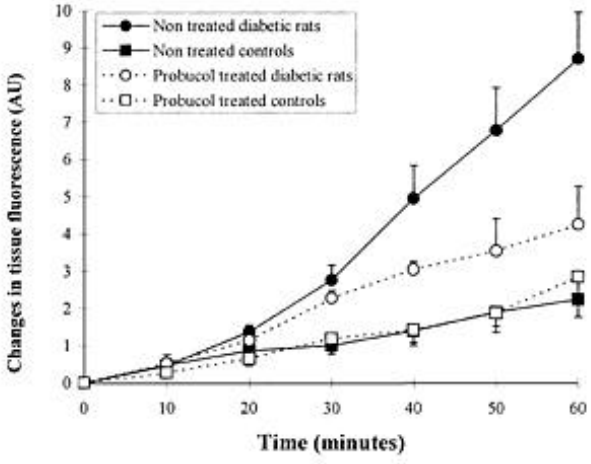


**FIG. 4. Effects of an intravenous bolus of antioxidant on diabetes-induced increases of microvascular albumin leakage. Diabetic rats and age-matched controls were studied 7 weeks after injection of STZ (70 mg/kg) or citrate buffer. Diabetic and age-matched normoglycemic rats were allocated to receive either probucol by a single intravenous infusion (30 µg/kg, dissolved in 1% ethanol, 0.3 ml), or saline, 1 h before the beginning of the experiment. Probucol partially inhibited the increase in FITC-albumin extravasation observed in diabetic rats ($P < 0.05$). The results are presented as means ± SE, with $n = 6$ for probucol-treated diabetic rats and controls, respectively, and $n = 10$ and 15 for untreated diabetic rats and controls, respectively.**

**Immunostaining of RAGE.** As shown in Fig. 5, RAGE was detectable by immunostaining in cremasteric vessels and was increased in diabetic rats versus age-matched controls.

## DISCUSSION

By using intravital fluorescence microscopy, the present study allowed us to assess the role of AGE–RAGE interaction in the vessel wall in diabetes-associated changes in macromolecular transendothelial transport at the microvascular level.

**Methodological considerations.** Laux and Seiffge (25) have demonstrated that mediator-induced changes in microvascular permeability can be quantified by using analysis of gray value distribution after computerization of the fluorescence image of the microvascular network. The same principles were used in the present study. However, contrasting with studies using application of mediators, we did not observe any leakage sites but rather a generalized diffusion from the entire microvascular network studied. Indeed, the present results reflected changes in the basal level of albumin transport rate across the microvascular wall rather than changes in the acute response to permeability mediators as in the cited study (25). Even when leakage sites are absent, permeability can vary from one vessel to another, or in different parts of the same vessel. It is the reason why, in the present study, we decided to consider measurements made on a relatively large area in order to limit the risk of biased extrapolations coming from the selection of particular vessels.

Note that the fluorescence intensity obtained in the first set of experiments was lower than that obtained in the other three sets, likely due to differences in batches of fluorescent albumin. Indeed, when the same batch of albumin was used (i.e., in experimental sets 2, 3, and 4), we found no significant difference in fluorescence measurements among the three groups of diabetics without treatment, or among three groups of nondiabetic rats. From a methodological point of view, this observation stressed the absolute necessity of comparing in all cases diabetic-treated animals with their nondiabetic and diabetic untreated controls using the same batch of FITC-albumin. This is the reason why these control groups were used in each set of experiments.

The measurements issued from tracer extravasation are commonly extrapolated to permeability measurements. It should be noted, however, that vascular density affecting exchange surface area can also affect macromolecular transport. First, we have checked in the four sets of experiments that the percentage of vascular area ($A\%_{vasc}$) in the studied area was similar in diabetic versus normoglycemic rats ($P > 0.5$ in all series of experiments). In addition, we carried out experiments comparing capillary density in diabetic and control rats. The absence of any significant difference made it unlikely that the difference in macromolecular transport was due to differences in exchange-surface area. These conclusions are similar to those found by others in rats (27,28) and patients (29), but not in mice (30). In patients, the possibility that an increase in blood flow from the loss of autoregulation can increase microvascular pressure and by this mechanisms increase macromolecule extravasation has also been proposed. However, in STZ-treated rats after 7 weeks of diabetes, Sexton et al. did not find any increase in capillary or venous pressure (28). In addition, in the same model in preliminary experiments we did not find any increase in microvascular blood flow (data not shown), and in diabetic mice Bohlen and Niggl (30) found blood flow marginally decreased. For these reasons, it seems likely that the increase in albumin microvascular leakage observed here was attributable to an increase in permeability to macromolecules.

**Mechanisms involved in the increase in albumin microvascular leakage.** Hyperglycemia during diabetes leads to the formation of irreversible AGEs. AGEs are involved in the development of vascular complications of diabetes and act to enhance protein and lipoprotein deposition and cause expansion of extracellular matrix components (31). These phenomena are generally defined as "long-term" changes in diabetic vessels. However, the main results of the present study (obtained 1 h after rR-RAGE intravenous administration) shows that, in vivo, inhibition of AGE–RAGE interaction can acutely inhibit microvascular hyperpermeability found in experimental diabetes. In addition, it should be noted that we did not observe an additional decrease in permeability when rats were studied 3 or 12 h after the

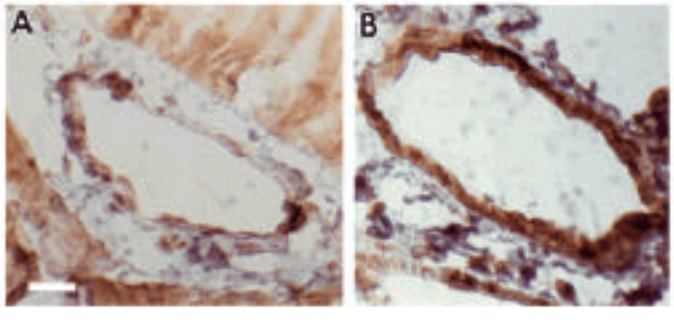


**FIG. 5. RAGE in cremaster muscle vasculature. Immunostaining of RAGE in a vessel from cremaster muscle of a control rat (*A*) versus a diabetic rat (*B*). Diabetic rats and age-matched controls were studied 7 weeks after injection of STZ (70 mg/kg) or citrate buffer. Scale bar represents 20 µm.**

rR-RAGE intravenous administration, thus showing that the rR-RAGE effect did not have a long time-lag before its maximal effect. The involvement of RAGE in the acute modulation of permeability is also confirmed by the inhibition of albumin extravasation by anti-RAGE antibody. Taken together, these findings suggest that permeability at the microvascular level is continuously upregulated via an AGE-RAGE–dependent mechanism, and that this mechanism is rapidly reversible (at least partially).

The rapidity of this reversibility strongly suggests that hyperpermeability involves not only structural changes but is also largely dependent on functional changes.

Taken together, these results obtained by in vivo videomicroscopy in muscle also confirm those obtained by whole-organ experiments by Wautier et al. (23).

Consistent with earlier studies demonstrating enhanced expression of RAGE in diabetic vasculature (17), increased expression of RAGE in cremaster muscle retrieved from diabetic rats was noted compared with that in age-matched euglycemic controls. The possibility that oxidant stress can modulate permeability in experimental diabetes is also suggested by the present results showing that the antioxidant drug probucol reduces albumin extravasation in diabetic animals. Such a mechanism has been previously reported by Shasby et al. (32), showing that an oxidative stress can reversibly increase endothelial permeability to macromolecules by rapid changes in endothelial cell shape via $Ca^{2+}$-mediated mechanisms (22,32). Reactive oxygen species can also increase permeability by quenching nitric oxide (33). Indeed, decrease in NO has been reported to increase microvascular permeability by direct mechanisms (34,35) or via an increase in leukocyte sticking and activation (36,37). Note, however, that such mechanisms are still largely controversial since other authors have shown that NO potentiates rather than inhibits vascular permeability (10,12,38).

We reported that in the present model, blockade of RAGE, employing either soluble RAGE or anti-RAGE IgG or reduction in oxidant stress by probucol, inhibited hyperpermeability in diabetic rats. It has been previously demonstrated that incubating endothelial cell with AGE albumin leads to generation of oxidant stress (17). In addition, infusion of rR-RAGE in diabetic rats decreased oxidant stress determined by measurement of thiobarbituric acid–reactive substances (26) and decreased hyperpermeability induced by infusion of red cells from diabetic rats (23). Consequently, it is possible that the acute mechanism that modulates hyperpermeability in the present experiments could also involve RAGE-dependent, oxidant-sensitive pathways. However, further studies would be necessary for a direct demonstration of this mechanism.

In conclusion, the present study has shown that the increase in microvascular leakage of macromolecules in STZ-induced diabetic rats can be acutely decreased by soluble RAGE or anti-RAGE antibody. These results strongly suggest that in experimental diabetes the interaction of circulating AGEs and endothelial RAGE modulates microvascular permeability, possibly via oxidant-sensitive pathways.

## REFERENCES


1. Viberti GC: Increased capillary permeability in diabetes mellitus and its relationship to microvascular angiopathy. *Am J Med* 75:81–84, 1983
2. Shostak A, Gotloib L: Increased peritoneal permeability to albumin in streptozotocin diabetic rats. *Kidney Int* 49:705–714, 1996
3. Williamson JR, Chang K, Tilton RG, Prater C, Jeffrey JR, Weigel C, Sherman WR, Eades DM, Kilo C: Increased vascular permeability in spontaneously diabetic BB/W rats and in rats with mild versus severe streptozocin-induced diabetes. *Diabetes* 36:813–821, 1987
4. Alpert JS, Coffman JD, Balodimos MC, Koncz L, Soeldner JS: Capillary permeability and blood flow in skeletal muscle of patients with diabetes mellitus and genetic prediabetes. *N Engl J Med* 286:454–460, 1972
5. Jaap AJ, Shore AC, Tooke JE: Differences in microvascular fluid permeability between long-duration type I (insulin-dependent) diabetic patients with and without significant microangiopathy. *Clin Sci* 90:113–116, 1996
6. Wardle EN: Vascular permeability in diabetics and implications for therapy. *Diabetes Res Clin Pract* 23:135–139, 1994
7. Parving H-H, Rossing N: Simultaneous determination of the transcapillary escape rate of albumin and IgG in normal and long-term juvenile diabetic subjects. *Scand J Clin Lab Invest* 32:239–244, 1973
8. Tooke JE: Microvasculature in diabetes. *Cardiovasc Res* 32:764–771, 1996
9. Svensjö E, Arfors K-E, Raymond RM, Grega GJ: Morphological and physiological correlation of bradykinin-induced macromolecular efflux. *Am J Physiol Heart Circ Physiol* 5:H600-H606, 1979
10. Mayhan WG: Nitric oxide accounts for histamine-induced increases in macromolecular extravasation. *Am J Physiol Heart Circ Physiol* 266:H2369–H2373, 1994
11. Ialenti A, Ignaro A, Moncada S, Di Rosa M: Modulation of acute inflammation by endogenous nitric oxide. *Eur J Pharmacol* 211:177–182, 1992
12. Ramírez MM, Kim DD, Durán WN: Protein kinase C modulates microvascular permeability through nitric oxide synthase. *Am J Physiol Heart Circ Physiol* 271:H1702–H1705, 1996
13. Schmidt A-M, Hori O, Brett J, Yan SD, Wautier J-L, Stern D: Cellular receptors for advanced glycation end products: implication for induction of oxidant stress and cellular dysfunction in the pathogenesis of vascular lesions. *Arterioscler Thromb* 14:1521–1528, 1994
14. Gugliucci A, Bendayan M: Reaction of advanced glycation endproducts with renal tissue from normal and streptozotocin-induced diabetic rats: an ultrastructural study using colloidal gold cytochemistry. *J Histochem Cytochem* 43:591–600, 1995
15. Schmidt A-M, Yan SD, Stern D: The dark side of glucose. *Nat Med* 1: 1002–1004, 1995
16. Soulis T, Thallas V, Youssef S, Gilbert RE, McWilliam BG, Murray-Mcintosh RP, Cooper ME: Advanced glycation end products and their receptors co-localise in rat organs susceptible to diabetic microvascular injury. *Diabetologia* 40:619–628, 1997
17. Yan SD, Stern D, Schmidt AM: What's the RAGE? The receptor for advanced glycation end products (RAGE) and the dark side of glucose. *Eur J Clin Invest* 27:179–181, 1997
18. Wautier J-L, Wautier M-P, Schmidt AM, Anderson GM, Hori O, Zoukourian C, Capron L, Chappey O, Yan S-D, Brett J, Guillausseau PJ, Stern D: Advanced glycation end products (AGEs) on the surface of diabetic erythrocytes bind to the vessel wall via a specific receptor inducing vascular stress in the vasculature: a link between surface-associated AGEs and diabetic complications. *Proc Natl Acad Sci U S A* 91:7742–7746, 1994
19. Yan SD, Schmidt AM, Anderson GM, Zhang JH, Brett J, Zou YS, Pinsky D, Stern D: Enhanced cellular oxidant stress by the interaction of advanced glycation end products with their receptors/binding proteins. *J Biol Chem* 299: 9889–9897, 1994
20. Baynes JW: Role of oxidative stress in development of complications in diabetes. *Diabetes* 40:405–412, 1991
21. Giugliano D, Ceriello A, Paolisso G: Oxidative stress and diabetic vascular complications. *Diabetes Care* 19:257–267, 1996
22. Siflinger-Birnboim A, Lum H, Del Vecchio PJ, Malik AB: Involvement of $Ca^{2+}$ in the $H_2O_2$-induced increase in endothelial permeability. *Am J Physiol Lung Cell Mol Physiol* 270:L973–L978, 1996
23. Wautier J-L, Zoukourian C, Chappey O, Wautier M-P, Guillausseau PJ, Cao R, Hori O, Stern D, Schmidt AM: Receptor-mediated endothelial cell dysfunction in diabetic vasculopathy: soluble receptor for advanced glycation end products blocks hyperpermeability in diabetic rats. *J Clin Invest* 97:238–243, 1996
24. Vicaut E, Stücker O: An intact cremaster muscle preparation for studying the microcirculation by in vivo microscopy. *Microvasc Res* 39:120–122, 1990
25. Laux V, Seiffge D: Mediator-induced changes in macromolecular permeability in the rat mesenteric microcirculation. *Microvasc Res* 49:117–133, 1995
26. Renard C, Chappey O, Wautier M-P, Nagashima M, Lundh E, Morser J, Zhao L, Schmidt A-M, Scherrmann J-M, Wautier J-L: Recombinant advanced glycation end product receptor pharmacokinetics in normal and diabetic rats. *Mol Pharmacol* 52:54–62, 1997
27. Sexton WL: Skeletal muscle vascular transport capacity in diabetic rats. *Diabetes* 43:225–231, 1994
28. Sexton WL, Poole DC, Mathieu-Costello O: Microcirculatory structure-

function relationships in skeletal muscle of diabetic rats. *Am J Physiol Heart Circ Physiol* 266:H1502–H1511, 1994
29. Leinonen H, Matikainen E, Juntunen J: Permeability and morphology of skeletal muscle capillaries in type 1 (insulin-dependent) diabetes mellitus. *Diabetologia* 22:158–162, 1982
30. Bohlen HG, Niggl BA: Early arteriolar disturbances following streptozotocin-induced diabetes mellitus in adult mice. *Microvasc Res* 20:19–29, 1980
31. Brownlee M: Glycation products and the pathogenesis of diabetic complications. *Diabetes Care* 15:1835–1843, 1992
32. Shasby DM, Lind SE, Shasby SS, Goldsmith JC, Hunninghake GW: Reversible oxidant-induced increases in albumin transfer across cultured endothelium: alterations in cell shape and calcium homeostasis. *Blood* 65:605–614, 1985
33. Bucala R, Tracey KJ, Cerami A: Advanced glycosylation products quench nitric oxide and mediate defective endothelium-dependent vasodilatation in experimental diabetes. *J Clin Invest* 87:432–438, 1991
34. Kubes P, Granger DN: Nitric oxide modulates microvascular permeability. *Am J Physiol Heart Circ Physiol* 262:H611–H615, 1992
35. Oliver JA: Endothelium-derived relaxing factor contributes to the regulation of endothelial permeability. *J Cell Physiol* 151:506–511, 1992
36. Jahr J, Grände PO: In vivo effects of tumor necrosis factor-a on capillary permeability and vascular tone in a skeletal muscle. *Acta Anaesthesiol Scand* 40:256–261, 1996
37. Sims DE, Miller FN, Donald A, Horne MM, Edwards MJ: Interleukin-2 alters the positions of capillary and venule pericytes in rat cremaster muscle. *J Submicrosc Cytol Pathol* 26:507–513, 1994
38. Mayhan WG: Role of nitric oxide in modulating permeability of hamster cheek pouch in response to adenosine 5′-diphosphate and bradykinin. *Inflammation* 16:295–305, 1992